Automatic Creation of Synthetic Finite Element Seats Using Statistical Models

Pablo Gracia Cemborain, Daniel Hall, John Paul Donlon, Ayush Mehta, Bronislaw Gepner,
Adrian Caudillo-Huerta, Daniel Perez-Rapela, Marcy Edwards, Jessica Jermakian, Jason Forman

Abstract Finite element (FE) studies of rear-impact occupant response often rely on a single seat model, which limits the study of seat design variability. This work developed a largely automated workflow to generate synthetic FE seat variants based on measured production seat geometry. A total of 27 production seats were digitised and reduced to standardised descriptors of seat-back foam shape (27 seats), head restraint foam shape (24 seats) and internal dimensions (seven seats). Separate principal component analysis (PCA) models were trained for these three descriptor groups and sampled within bounded ranges to create synthetic target designs. These targets were then used to morph the OpenVT Driver Seat model through an ANSA-based process. The workflow generated 40 synthetic seat variants within the learned statistical design space. The generated seats passed pre-processing, penetration and mesh quality checks and were exercised in rear-impact simulations as a numerical usability demonstration. The generated seats are intended to reflect the geometric variability derived from the collected seat sample and to support exploratory studies requiring multiple geometrical seat configurations.

Keywords Finite element model, Morphing, Principal component analysis, Rear impact, Seat modelling.

I. INTRODUCTION

Vehicle seat design is an established factor influencing whiplash injury outcomes in rear impacts. Field studies have shown that advanced seat protection systems can reduce whiplash injury risk by approximately half compared to standard seats [1], although the Euro NCAP whiplash test protocol revealed wide variability in seat performance across the market [2]. Early work on the Whiplash Protection System (WHIPS) demonstrated that seat design characteristics directly influence occupant loading in rear impacts [3]. These findings confirm that seat design variability is a relevant factor when studying occupant response, yet finite element (FE) studies of rear impact have typically relied on one or a small number of seat models [4-5]. As a result, current FE practice is limited in its ability to examine how variation in seat design may influence occupant response.

Early simulation work used simplified multi-body seat representations [6], while later studies developed generic FE seat models to serve as open source tools [4]. Detailed FE models of individual production seats have also been developed for specific research purposes [5]. However, once again these efforts produced a single seat model or a small set of them. Linder *et al.* [7] reported different occupant response metrics for two different seat configurations under the same rear-impact pulse and highlighted the need to evaluate a wider range of seat designs, while showing that access to detailed commercial seat models remains limited. Parametric studies have explored the influence of selected seat design variables, such as stiffness, head restraint height and backset, on whiplash injury metrics [8-9], but these studies varied model parameters on simplified seat representations rather than generating new seat geometries from measured production seat data. More recent work has introduced parametric FE vehicle interiors with diverse occupant populations [10] and generic vehicle bucks developed from laser scans of multiple vehicles [11]. However, in these studies the seat geometry itself was not modified through a statistical model of seat design.

Mesh morphing techniques are well established for generating diverse FE human body model (HBM) populations. Radial basis function methods have been used to morph whole-body models across a wide range of body dimensions [12] and these approaches have enabled large-scale population studies with 100 morphed occupant models for crash simulation [13]. However, HBM morphing relies on anatomical landmark correspondence and anthropometric target databases that do not exist for vehicle seats. Seats combine

P. Gracia Cemborain (e-mail: fmx7jf@virginia.edu; tel: +1 434-297-8037) is a Research Engineer, D. Hall is a Postdoctoral Research Associate,, J.-P. Donlon is a Senior Research Specialist, A. Mehta is a Graduate Research Assistant, B. Gepner is a Senior Research Scientist, A. Caudillo-Huerta is a Research Engineer and J. Forman is a Principal Investigator, all at the University of Virginia, USA. D. Perez-Rapela is an Owner and Consultant at Human Injury Consulting and Research LLC. M. Edwards is a Senior Research Engineer and J. Jermakian is the Vice President of Vehicle Research at the Insurance Institute for Highway Safety (IIHS).

continuous foam surfaces with discrete internal structural components, which complicates the definition of a single deformation procedure capable of preserving both exterior geometry and internal structure. PCA-based approaches to generating FE model populations from measured geometry have been demonstrated in human body modelling, where measured specimens are used to train a PCA model, which extracts the dominant geometric variations and from which synthetic instances can be sampled to create new FE models [14]. To the best of the authors' knowledge, no prior work has reported combining a PCA-based statistical representation of production seat geometry with automated FE morphing to generate synthetic seat model populations.

The objective of this study was to develop a workflow to generate synthetic FE vehicle seat variants from a statistical representation of measured production seat geometry and internal dimensions.

The contribution of this work is an end-to-end automated process connecting physical seat digitisation, standardised geometric description, PCA-based statistical modelling, synthetic target generation and template morphing of the OpenVT Driver Seat [15] into simulation-ready FE seat variants. Forty synthetic seats were generated within the learned design space and exercised in rear-impact simulations as a numerical integrity demonstration. The generated seats are intended to reflect the geometric variability observed in the collected seat sample and to support exploratory simulation studies requiring many seat configurations.

II. METHODS

A. Physical seat dataset

A total of 27 production seats were collected from the US market through the Insurance Institute for Highway Safety (IIHS), approximately from model years 2008 to 2022. The collection intentionally sought visible variability in seat design, including seats with different overall dimensions, seats with and without lumbar support-related internal features, and seats with separate head restraints and seats with integrated head restraints.

Exterior foam surfaces were digitised for all collected seats, yielding 27 seat back and 24 head restraint shape entries after three head restraint scans were excluded due to insufficient scan quality. Internal structural measurement required destructive removal of the seat foam and manual digitisation of discrete reference points on the exposed frame. This procedure was applied to a subset of seven seats, resulting in seven entries for the internal dimensions dataset.

Integrated head restraint seats were included in the scanned dataset and therefore contributed to the statistical representation of exterior seat geometry. However, the FE template model used in this study represents a non-integrated head restraint architecture. Consequently, while the statistical models reflect variability observed in both architectures, the generated FE seat variants correspond only to the non-integrated head restraint configuration of the template model.

B. Standardised geometric descriptors

Three categories of seat information were captured: seat-back exterior foam geometry; head restraint exterior foam geometry; and internal structural reference points. Prior to scanning and internal measurement, the seats were received from IIHS in the configuration used for its seat/head-restraint evaluation procedures for rear-impact testing. In the dynamic protocol [16], seat adjustments are standardised and BioRID positioning is based on reference measurements made with the H-point machine and Head Restraint Measuring Device (HRMD), with the seatback adjusted to support a 24-26 degree torso angle. Therefore, the internal frame angle A1 was measured in the IIHS-prepared rear-impact test configuration rather than from an arbitrary recliner adjustment position.

The internal structural reference points were used to calculate discrete geometric measurements and identify the presence of lumbar support region structures (see Figure 1). The geometric scope of the study was limited to the seat back and head restraint regions. The seat pan and lower anchor or rail regions were largely excluded from the statistical representation, except where width modification was required during FE morphing to maintain geometric proportions. Internal reference points were digitised and later converted into discrete geometric measurements describing the internal structure of the seat back and head restraint (see Figure 2). The presence of lumbar support region structures was represented using three binary variables corresponding to the top, middle, and bottom lumbar support regions of the template model.

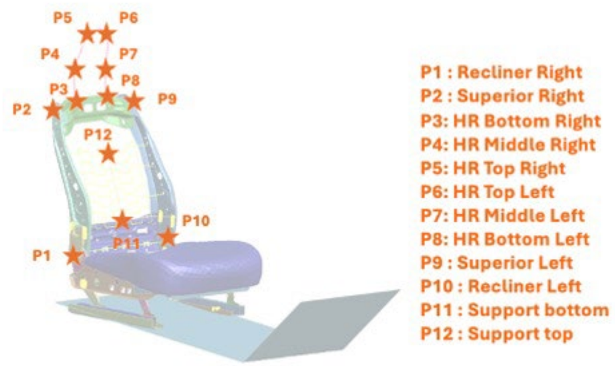

Fig. 1. Digitised internal reference points on seat.

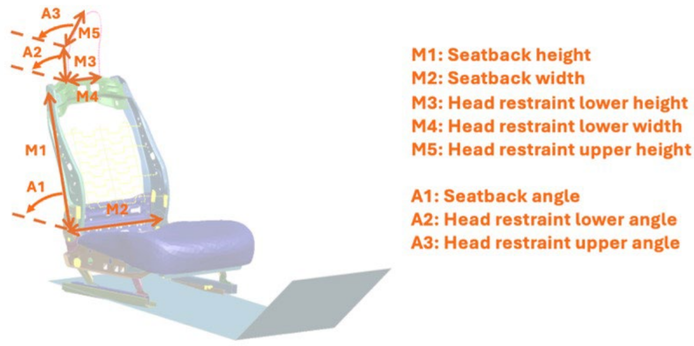

Fig. 2. Resultant geometric measurements on seat.

C. Point cloud standardisation

The exterior surface of each seat was digitised using a 3D scanner (Absolute Arm 8330-7 with RS5 V2 Scanner, Hexagon Manufacturing Intelligence, Kingstown, RI, USA). The front portions of the head restraint and seat back were extracted from the scans and post-processed in a reverse engineering software (Geomagic Design X, Hexagon Manufacturing Intelligence, Kingstown, RI, USA) to create closed single-manifold surfaces with a uniform mesh density consistent across all seats and extraneous features removed (e.g. tags and head restraint height-adjustment hardware). Surfaces were aligned to a consistent reference frame, with the origin at the centre of the bight, the Z-axis positive vertically up, the Y-axis positive to the right, and the X-axis positive rearward. Here, the bight refers to the transition region between the seat-back and seat-pan cushions. It was used as a surface-based alignment landmark rather than the H-point because the purpose of this step was to orient the scanned seat-back surface for horizontal cast projection, whereas the H-point is a reference located away from the scanned seat-back surface and would produce a forward-tilted alignment with respect to the desired projection direction. Surfaces were exported as stereolithography (.STL) files containing the vertices and facet triangulation describing the surfaces. These were then standardised with Python through a semi-automated procedure applied separately to the seat back and head restraint. This standardisation reduced scan-produced differences introduced during manual digitisation before the casts were used for PCA, so the statistical models represented surface-shape variation rather than differences in scan orientation. User intervention was limited to threshold selection during pre-processing and review of intermediate outputs.

For each scan the following standardisation procedure was applied (see also Appendix A).

1. Read the point cloud.
2. Remove loose points not connected to the main geometry.
3. Align the scan frontally by identifying the most forward points on both lateral sides of the seat surface and rotating to remove the yaw angle between them.
4. Align the scan vertically by estimating the pitch angle from the bight and the transition between the bolster and central regions of the seat-back surface, then rotating the scan to remove this angle.
5. Isolate the most forward seat surface using a depth threshold to retain only the front-facing portion of the geometry intended for morphing. A lower depth threshold retains a smaller, more anterior portion of the surface, while a higher threshold can include side or rear facing regions of the seat.
6. Retain faces oriented toward the front using an angular threshold.
7. Position a regular 10 by 10 planar grid, referred to as the cast, in front of the target surface. The cast is a standardised set of 100 equally spaced points used to create a common geometric representation across all scanned seats.
8. Project the cast points onto the seat surface. For each cast point, if the perpendicular projection fell within the seat surface contour, the point was projected to the nearest location on the scan along the projection direction. If the perpendicular projection fell outside the contour, the point was assigned to the closest scan point based on lateral and vertical distance.
9. Restore the cast to the original seat orientation.

This procedure reduced each seat region to a standardised 100-point cast. Alternative grid resolutions were evaluated, including 50 and 1,000 points. A resolution of 50 points provided insufficient geometric detail to capture relevant surface features, while 1,000 points introduced excessive constraint during the morphing process. A resolution of 100 points was selected as a practical balance between geometric fidelity and morphing complexity. Point correspondence between seats was derived from the common cast structure, with points numbered consistently from left to right and top to bottom. The empirical thresholding stages were important to isolate the front surface intended for morphing and to prevent cast projection onto unintended rear-facing regions.

D. Statistical representation of seat geometry

Separate PCA models were created for seat-back foam shape (27 seats), head restraint foam shape (24 seats) and internal geometric measurements (7 seats). The seat back and head restraint models were built from the standardised 100-point surface casts (see Figure 3 and Figure 4), while the internal dimensions model was built from the measured geometric variables of the subset of seats (see Figure 2).

PCA was selected because it provided a transparent low dimensional statistical representation suitable for parameter bounding and for generating new geometric instances by sampling weight combinations within the learned space. Separate PCA models were used for each component due to practicality and modularity. A single combined model would have mixed high dimensional surface coordinate data with low dimensional scalar measurements, making normalisation, weighting, interpretation and later morphing control overly complex. Separate models also allowed independent combination of seat back and head restraint designs. The trade-off was that correlations between both exterior shapes and the internal dimensions were not explicitly preserved.

Prior to PCA, the exterior surface casts were geometrically aligned to a common reference by removing residual frontal and vertical misalignment using stored pre-processing parameters from the point cloud standardisation step and translating each cast so that its centroid coincided with the coordinate origin. The aligned casts were then vectorised and used as input to PCA, ensuring that the analysis captured shape variation rather than positional or orientational differences. PCA was applied directly to the aligned coordinate vectors without scaling, since all coordinates shared the same physical unit. For the internal dimensions model, variables were standardised to zero mean and unit variance prior to PCA to remove scale differences between angular and linear measurements.

Due to the limited number of seats available for the internal dimensions model, this PCA serves primarily as a compact parameterisation of the observed dimensional ranges rather than as a statistical representation of the broader seat population. The exterior shape models, trained on 27 and 24 seats respectively, provide a more robust statistical reference.

The number of retained PCA dimensions was selected to capture at least 70% of the explained variance in each model. A higher variance threshold was considered, but would have required additional retained components, increasing the parameter count and introducing localised deformations that were handled less robustly by the morphing pipeline. The 70% threshold was therefore selected as a practical compromise between variance capture, parameter space dimensionality and morphing robustness.

Synthetic target designs were generated by sampling PCA weights within bounded ranges. The weights were limited to plus and minus one standard deviation and drawn from uniform distributions within that range. These bounds were selected to reduce the occurrence of extreme combinations that produced visually unrealistic geometries while still allowing broad exploration of the learned design space.

E. Reference FE seat model

The OpenVT Driver Seat was used as the template FE model for morphing. This model was selected because it is an openly available FE seat model that was considered suitable for the present automated geometry modification workflow. All generated seats therefore inherit the structural architecture of the OpenVT template, including its separate seat back and head restraint configuration. As a result, the generated set did not include FE representations of integrated head restraint designs, even though such seats contributed to the statistical model.

Prior to morphing, the base FE model was modified to split the original single lumbar support part into three separate support regions: top, middle, and bottom. This pre-processing step was necessary so that during the morphing workflow individual support regions could be kept or deleted as needed to match the target design, controlling the presence, absence or extent of lumbar support features as a binary design variable.

F. Automated morphing workflow and implementation

The sampled statistical targets were converted into FE seat variants through a largely automated ANSA 23 morphing workflow. At a high level the procedure's steps are (see also Appendix B):

1. Generate target seat-back and head restraint shape casts and seat internal dimensions from PCA models.
2. Calculate deformation maps between template casts and target casts. Each deformation map was defined as the displacement field between corresponding cast points on the template and the synthetic target.
3. Import the OpenVT FE seat into ANSA.
4. Morph the seat-back and head restraint foam geometry in ANSA using the deformation maps derived from the cast correspondence.
5. Apply internal dimensional changes to the seat-back and head restraint structures using ANSA direct morphing.
6. Perform smoothing and local cleanup operations.
7. Delete or keep lumbar support regions as needed to match the target design.
8. Remesh the foam regions.
9. Save the resulting FE seat model together with diagnostic outputs.

Throughout the template-based morphing process, the original model connectivity, contacts and constraints were preserved. Local dimensional changes were propagated to adjacent parts, where necessary, to maintain geometric continuity. This included width adjustments in the seat pan and lower anchor regions, which were not included in the PCA models but were required to maintain overall geometric proportions during morphing.

G. Process automation and quality control

The full workflow was automated with Python, including scan pre-processing, cast generation, PCA training, target generation, deformation map calculation and ANSA process control for morphing. The workflow was organised in stages so that intermediate outputs, including cast generation, deformation map calculation, PCA training and final FE morphing, could be inspected independently. The main user inputs for seat generation were the scan pre-processing thresholds and the PCA weights defining the target geometry. Runtime was on the order of a few minutes per generated seat, with the ANSA morphing and remeshing stages acting as the main bottlenecks.

Quality control was applied at three stages.

1. ANSA-based penetration and mesh quality checks during morphing, using default ANSA quality criteria.
2. Successful solver deployment in rear-impact FE simulations.
3. Expert visual review of geometric realism.

At the simulation stage, acceptable behaviour was defined as the absence of large non-physical deformation or loss of structural continuity attributable to the morphing process. This criterion, together with the visual review, was qualitative. Since the generated seats are novel geometries with no physical counterpart, no ground truth reference exists against which to evaluate them and no established acceptance thresholds exist for geometric deviation in synthetic FE seat models. Defining quantitative acceptance criteria remains an open task.

Forty generated seats were exercised in rear-impact FE simulations using LS-DYNA as a numerical integrity demonstration. These seats were exercised in four different pulses severities generating a total of 160 simulations. These were not intended as validation of the generated seats against physical seats or response corridors. Their role was to verify that the morphing procedure produced FE models that could be deployed in rear-impact simulations without obvious numerical problems attributable to the generated seat models.

The simulation environment included the morphed seat, a BioRID II FE dummy and a simple seat belt under rear-impact conditions with four severities. The included pulses were [2]:

- IIWPG (16 km/h);
- NCAP Low (16 km/h);
- NCAP High (24 km/h);
- JNCAP (20 km/h).

III. RESULTS

Exterior foam surfaces from 27 seat-back and 24 head restraint scans were processed into standardised casts (see Figure 3 and Figure 4) suitable for statistical modelling after exclusion of low quality scans. Internal structural measurements were obtained for a subset of seven seats.

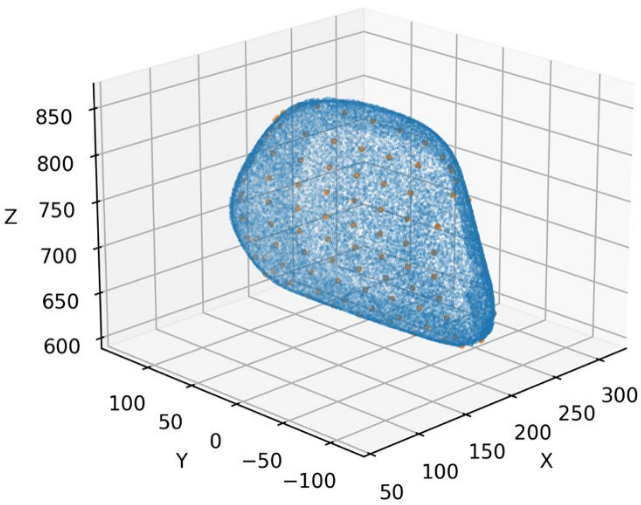

Fig. 3. Head restraint scan with cast.

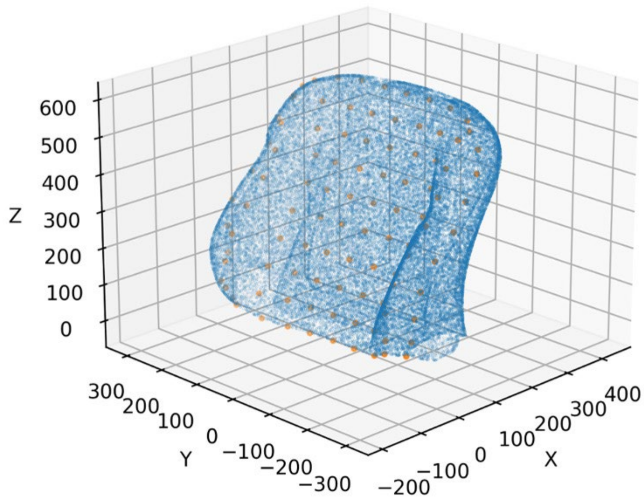

Fig. 4. Seat-back scan with cast.

Separate PCA models were constructed for seat-back exterior shape, head restraint exterior shape and internal dimensions. Scree plots show that the majority of variance is captured within the first three to four components for all models (Appendix C). The quantitative summary of these scree plots, including the retained number of PCs and corresponding explained variance, is provided in Table I.

TABLE I

SUMMARY PCA RETAINED PCS AND EXPLAINED VARIANCE

PCA Model	N	PCs retained	Explained variance (%)
Seat-back exterior shape	27	4	72.50
Head restraint exterior shape	24	3	78.50
Internal dimensions	7	3	86.00

The retained components capture coupled geometric variations involving combinations of curvature, bolster depth and contour shape, with no single component corresponding to an isolated physical characteristic (Appendix D).

Reconstruction of original geometries using the retained components resulted in root mean squared error (RMSE) values lower than 4 mm and 10 mm for the head restraint and seat-back geometries, respectively. Deviations were primarily local and more pronounced in the edge regions, while overall shape fidelity was preserved (Appendix E).

The internal dimensions model shows comparatively higher explained variance, as shown in Table I. However, this should be interpreted in the context of the limited dataset size. The internal dimensions PCA model acts as a compact parameterisation of the observed internal measurements rather than a statistically robust population model. The generated samples populate the internal dimensions design space within the defined plus and minus one standard deviation bounds, as shown in Figure 5. The resulting distributions show that the measured dataset captures a limited number but large range of seat geometries, while generated parameter sets follow similar central tendencies and provide more continuous coverage of the bounded internal dimensions design space.

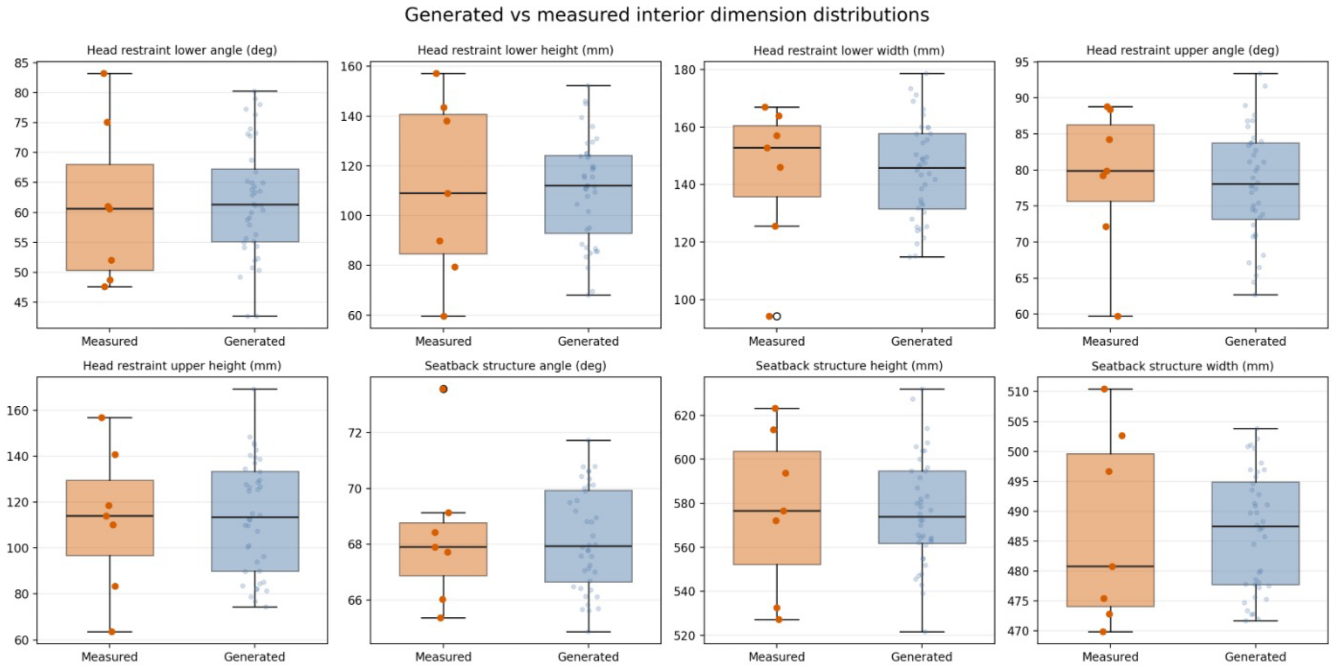

Fig. 5. Generated vs measured interior dimension distributions.

The automated workflow generated 40 synthetic FE seat models spanning a bounded design space defined by the retained PCA modes and sampling within plus and minus one standard deviation. The morphing process produced geometrically coherent seat variants across this space, with continuous and stable shape transitions. Minor local artefacts, such as sharp edges, were occasionally introduced during morphing, typically concentrated in regions of rapid changing curvature, but remained limited in extent and did not affect overall geometry integrity or usability. Representative morphed seat variants are shown in Figure 6. The examples are labelled S1-S8 and their corresponding internal geometric descriptors are listed in Table II.

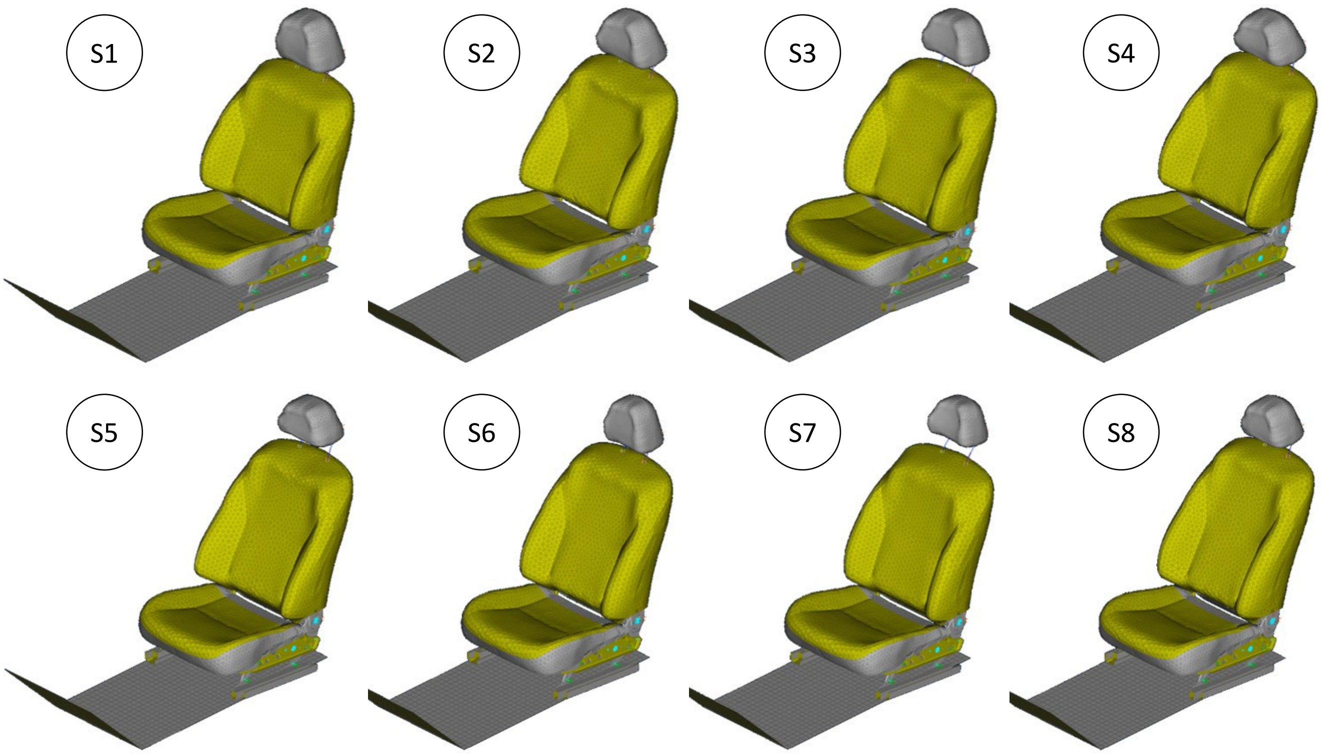

Fig. 6. Example morphed seats.

TABLE III

EXAMPLE MORPHED SEATS DIMENSIONS FROM FIGURE 6. LINEAR MEASUREMENTS M1-M5 ARE IN MM AND ANGULAR MEASUREMENTS A1-A3 ARE IN DEGREES, AS DEFINED IN FIGURE 2.

Seat	M1	M2	M3	M4	M5	A1	A2	A3
S1	531.2	499.1	106.4	149.2	137.5	71.5	52.3	100.0
S2	548.6	492.8	106.7	162.1	115.3	69.7	64.8	104.2
S3	553.0	501.9	127.7	158.7	107.2	71.0	54.4	95.3
S4	564.2	488.9	109.6	166.4	100.7	68.5	70.6	105.3
S5	601.8	485.9	126.3	153.6	82.4	67.2	67.0	99.1
S6	589.3	483.3	108.3	119.6	127.5	67.9	52.5	98.1
S7	600.4	491.6	134.3	132.9	98.5	68.6	51.2	91.3
S8	624.1	473.4	112.3	130.1	95.2	65.1	67.2	101.9

All generated seat models passed ANSA pre-processing checks, including penetration control and mesh quality requirements. The models were subsequently deployed in rear-impact simulations as a numerical integrity check. Forty generated seats were simulated under four loading conditions, generating 160 simulations in total. One simulation terminated early due to excessive BioRID dummy loading, associated with an extreme occupant response in that seat-pulse combination, rather than a numerical instability or morphing related artefact in the generated seat model. No systematic numerical instabilities attributable to the morphing process were observed, indicating that the generated seat models are numerically stable and directly usable in FE simulation environments. Representative simulation snapshots at the time of head contact are shown in Figure 7.

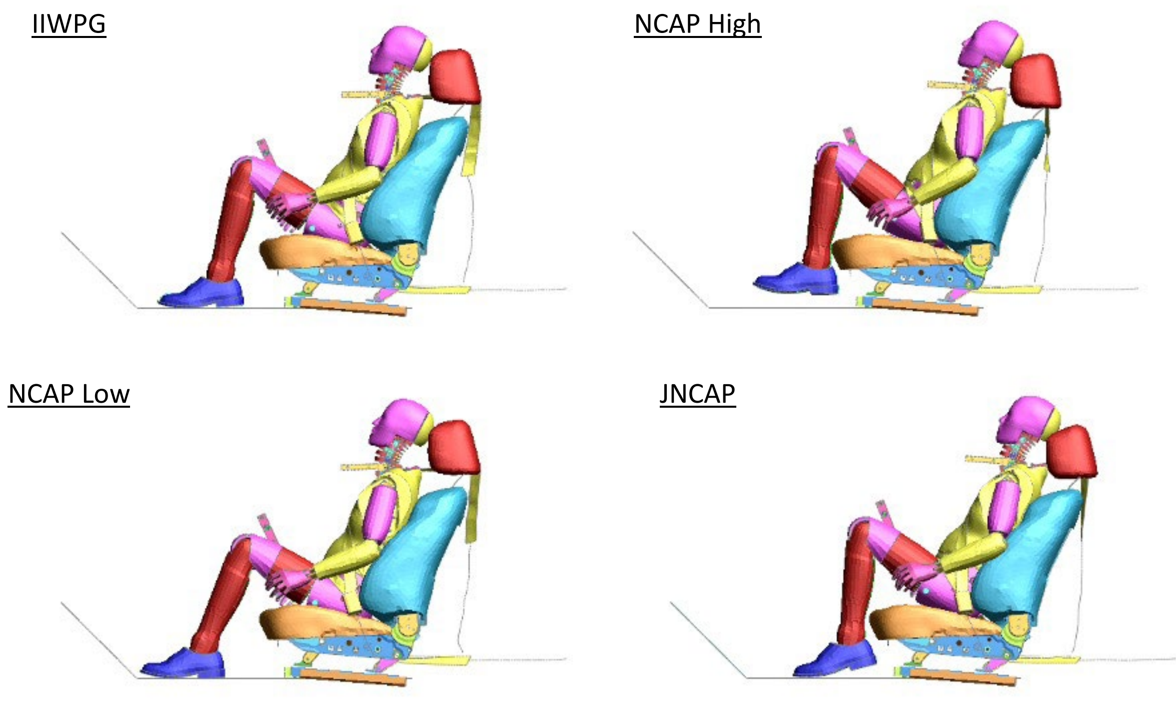

Fig. 7. Example morphed seat simulations at head-leaving-head restraint contact time.

IV. DISCUSSION

The main contribution of this work is that it provides a practical route to generate many geometries of varied FE seat models from measured production seat data. Previous FE studies in rear impact have generally relied on a single production seat model [5], a generic reference seat [4] or simplified parametric variation of a limited number of seat properties [8-9]. In contrast, the present workflow links physical measurement of production seats to the generation of multiple geometrically varied FE seat models on a common template. This makes it possible to treat seat geometry as a study variable rather than as a fixed boundary condition.

This approach follows the same general principle used in other areas of biomechanics, where measured geometries are reduced to a compact statistical representation and new instances are generated through sampling [14]. Similar strategies have also been used to morph FE models across a range of geometric variations and generate large model populations for simulation studies [12-13]. However, the seat problem introduces additional challenges. Vehicle seats lack a standardised landmark system, combine continuous foam surfaces with discrete internal structures, and are not supported by large reference databases. As a result, the present method adopts a mixed representation in which exterior surface geometry is described statistically, while selected internal frame dimensions are applied during morphing.

The scree plot summary in Table I shows that the retained components captured 72.5%, 78.5% and 86.0% of the variance for the seat-back, head-restraint and internal-dimensions models, respectively. This supported a reduced parameterisation in which the dominant observed variations were retained while limiting the number of morphing inputs required for automated model generation. The retained components should therefore be interpreted as a practical dimensionality reduction for robust seat generation, rather than as a complete description of all local geometric variation in the measured seats.

The use of three separate PCA models improved modularity and compatibility with the staged morphing process and avoided combining dense coordinate data with low dimensional scalar measurements in a single space. In this workflow, the seat-back and head-restraint exterior PCA models generated target foam surface shapes, while the internal dimensions PCA model generated the structural dimensions and angular measurements applied during morphing. This simplification comes at the cost of not preserving correlations between seat-back shape, head restraint shape and internal dimensions. Consequently, although the generated seats remained bounded within plus and minus one standard deviation of each individual PCA model, the independent sampling allowed combinations of features that were not present in any single measured seat. This was a deliberate exploratory choice to enable recombination of bounded component features, rather than to generate statistically representative production seats.

PCA components represent coupled modes of variation, so changing one PC score can modify several geometric features simultaneously. As a result, the PCA weights themselves are not equivalent to explicit seat design measurements such as head-restraint height, backset or seatback angle. This limits direct control of individual measurements and can make it difficult to isolate which specific geometric feature drives a change in crash response. However, conventional geometric measurements can be extracted from the generated seats after morphing, and occupant measures such as backset can be measured after dummy positioning with the generated seat designs. These measurements can then be related to simulation responses in subsequent analyses. In addition, the morphing pipeline could be driven directly by selected explicit measurements if a future study required controlled perturbation of those variables. Therefore, the present PCA-based parameterisation should be viewed as a geometry generation tool rather than as a causal parameterisation of individual injury relevant seat measurements.

A second key design choice was the reduction of each scanned surface to a standardised 100-point grid. This representation preserved the overall shape envelope, depth distribution and primary geometric features required for stable morphing, while maintaining a tractable parameterisation. However, it did not capture fine local geometric details such as sharp curvature transitions or small ergonomic features. The selected resolution should therefore be interpreted as a practical compromise between geometric fidelity and robustness of the automated morphing process.

Robust automatic morphing of the foam regions remained the most challenging part of the workflow. Surface smoothing, mesh smoothing and remeshing were necessary to prevent gross distortions and maintain model usability. In addition, some dimensional changes had to be propagated to adjacent regions outside the PCA-defined geometry, particularly the seat pan and lower anchor regions' width, to preserve overall geometric continuity. These steps show that, although the workflow was largely automated, practical morphing robustness still depended on empirically tuned post-processing operations.

The workflow is also dependent on the reference FE seat model used as a template. All generated seats inherit the topology, material definitions, contact formulations and boundary conditions of the OpenVT model. As a result, assumptions and simplifications present in the template are propagated to all generated variants. In addition, integrated head restraint configurations were not represented as distinct FE topologies, although they contributed to the statistical description of the dataset.

The study has further limitations related to dataset size, measurement scope and validation. The exterior shape models were trained on 27 seat-back and 24 head restraint scans, while the internal dimensions model relied on only seven seats for which destructive disassembly was performed. The internal dimensions PCA therefore captures the dimensional ranges of a small subset of seats rather than providing a robust statistical characterisation of the broader seat population. The collected sample was designed to capture variability rather than represent the full market distribution. The generated seats were evaluated primarily through pre-processing checks, simulation deployment and expert visual review. The present work therefore demonstrates numerical usability of the generated models within the stated workflow, but it does not establish physical validity or representativeness of a wider seat population.

Despite these limitations, the results show that generation of a synthetic FE seat population from measured production seat geometry is feasible within a bounded statistical design space. Forty seat variants were generated and most corresponding simulations completed normally, indicating that the workflow can support exploratory studies requiring many geometrically varied seat configurations.

Future work should focus on expanding the dataset, particularly the number of internally measured seats, developing quality metrics for seat morphing and coupling geometric variation with material and structural properties. The present workflow modifies seat geometry while preserving the structural architecture, material definitions, contacts and mechanisms of the OpenVT template model. Consequently, it does not independently control mechanical or structural properties such as cushion stiffness, spring behaviour, frame stiffness, recliner response, energy absorption or active/reactive head-restraint functionality. These properties are important for rear-impact biomechanics and may interact with geometric effects in some loading conditions. Coupling the present geometry morphing workflow with independent control of material and structural properties would allow future studies to distinguish the effects of seat geometry from those of mechanical properties and seat protection mechanisms. These extensions would move the method toward a more comprehensive representation of seat design variability, but they are not required to support the main finding of the study: that statistically driven generation of geometrically varied FE seat models on a common template is achievable.

V. CONCLUSION

Forty synthetic FE vehicle seat variants were generated from measured production seat geometry and internal dimensions through a workflow combining PCA-based statistical modelling and ANSA-based morphing of the OpenVT Driver Seat. The generated seats were bounded by the learned statistical design space of the collected sample and were exercised in rear-impact simulations as a numerical usability check. The framework therefore provides a practical way to generate many seat models of varied geometries from a common reference seat, while remaining limited to the geometry variation captured in the collected sample and to the structural architecture of the template model. The most valuable next step is to extend the framework to a larger and more representative seat dataset, particularly the internal dimensions measurements, and to incorporate variation in material and structural properties alongside geometry.

VI. ACKNOWLEDGEMENTS

This study was conducted jointly by the Insurance Institute for Highway Safety (IIHS) and the University of Virginia Center for Applied Biomechanics. The authors would like to thank DYNAmore, an ANSYS company, for the use of the BioRID FE model, BetaCAE for the use of ANSA software and the OpenVT project for the use of the OpenVT Driver Seat model. The authors also thank IIHS for providing the physical seats used in this study.

VII. REFERENCES

[1] Kullgren, A., Krafft, M., Lie, A., Tingvall, C. (2007) The effect of whiplash protection systems in real-life crashes and their correlation to consumer crash test programmes. *Proceedings of the 20th International*

Technical Conference on the Enhanced Safety of Vehicles, 2007, Lyon, France.

[2] van Ratingen, M., Ellway, J., *et al*. (2009) The Euro NCAP whiplash test. *Proceedings of the 21st International Technical Conference on the Enhanced Safety of Vehicles*, 2009, Stuttgart, Germany.

[3] Jakobsson, L., Lundell, B., Norin, H., Isaksson-Hellman, I. (1999) WHIPS - Volvo’s whiplash protection study. *Proceedings of the IRCOBI Conference*, 1999, Sitges, Spain.

[4] Genzel, J., Carlsson, A., Linder, A., Pipkorn, B., Svensson, M. (2022) An open-source finite element model of a generic car seat: Development and validation for low-severity rear impact evaluations. *Proceedings of the IRCOBI Conference*, 2022, Porto, Portugal.

[5] Bridges, W., Ganesan, V., Jayakumar, P., Davies, J., Paramasuwom, M. (2019) National Highway Traffic Safety Administration, Front seat modelling in rear impact crashes: Development of a detailed FE model for seat back strength requirements (Report No. DOT HS 812 737), Washington, D.C., USA.

[6] Eriksson, L. (2002) Three-dimensional mathematical models of the BioRID I and car seats, for low-speed rear-end impacts. *Traffic Injury Prevention*, **3**(1): pp. 75–87.

[7] Linder, A., Holmqvist, K., Svensson, M. Y. (2018) Average male and female virtual dummy model (BioRID and EvaRID) simulations with two seat concepts in the Euro NCAP low severity rear impact test configuration. *Accident Analysis & Prevention*, **114**: pp. 62–70.

[8] Viano, D. C. (2003) Seat properties affecting neck responses in rear crashes: A reason why whiplash has increased. *Traffic Injury Prevention*, **4**(3): pp. 214–227.

[9] Sendur, P., Thibodeau, R., Burge, J., Tencer, A. (2005) Parametric analysis of vehicle design influence on the four phases of whiplash motion. *Traffic Injury Prevention*, **6**(3): pp. 258–266.

[10] Boyle, K. J., Hu, J., Reed, M. P., Rupp, J. D. (2024) Development of parametric finite element vehicle and restraint models for occupant protection research. *Proceedings of the IRCOBI Conference*, 2024, Stockholm, Sweden.

[11] Iraeus, J., Lindquist, M. (2016) Development and validation of a generic finite element vehicle buck model for the analysis of driver rib fractures in real life nearside oblique frontal crashes. *Accident Analysis & Prevention*, **95**(Pt A): pp. 42–56.

[12] Zhang, K., Cao, L., *et al.* (2017) An automated method to morph finite element whole-body human models with a wide range of stature and body shape for both men and women. *Journal of Biomechanics*, **60**: pp. 253–260.

[13] Hu, J., Zhang, K., *et al.* (2019) Frontal crash simulations using parametric human models representing a diverse population. *Traffic Injury Prevention*, **20**(sup1): pp. S97–S105.

[14] Bryan, R., Nair, P. B., Taylor, M. (2009) Use of a statistical model of the whole femur in a large scale, multi-model study of femoral neck fracture risk. *Journal of Biomechanics*, **42**(13): pp. 2171–2176.

[15] OpenVT Consortium. "Open Access Front Seat Model". https://openvt.eu/fem/open-access-front-seat-model. [cited 18 March 2026].

[16] Insurance Institute for Highway Safety. (2019) Vehicle Seat/Head Restraint Evaluation Protocol, Dynamic Criteria (Version V). Insurance Institute for Highway Safety, Ruckersville, VA, USA. https://www.iihs.org/media/d71952c9-4e3a-4e43-ab6e-eae25f59972a/oRbIIA/Ratings/Protocols/current/head_restraint_protocol_dynamic.pdf. [cited 28 April 2026].

VIII. APPENDIX

Appendix A: Point Cloud Standardisation Procedure

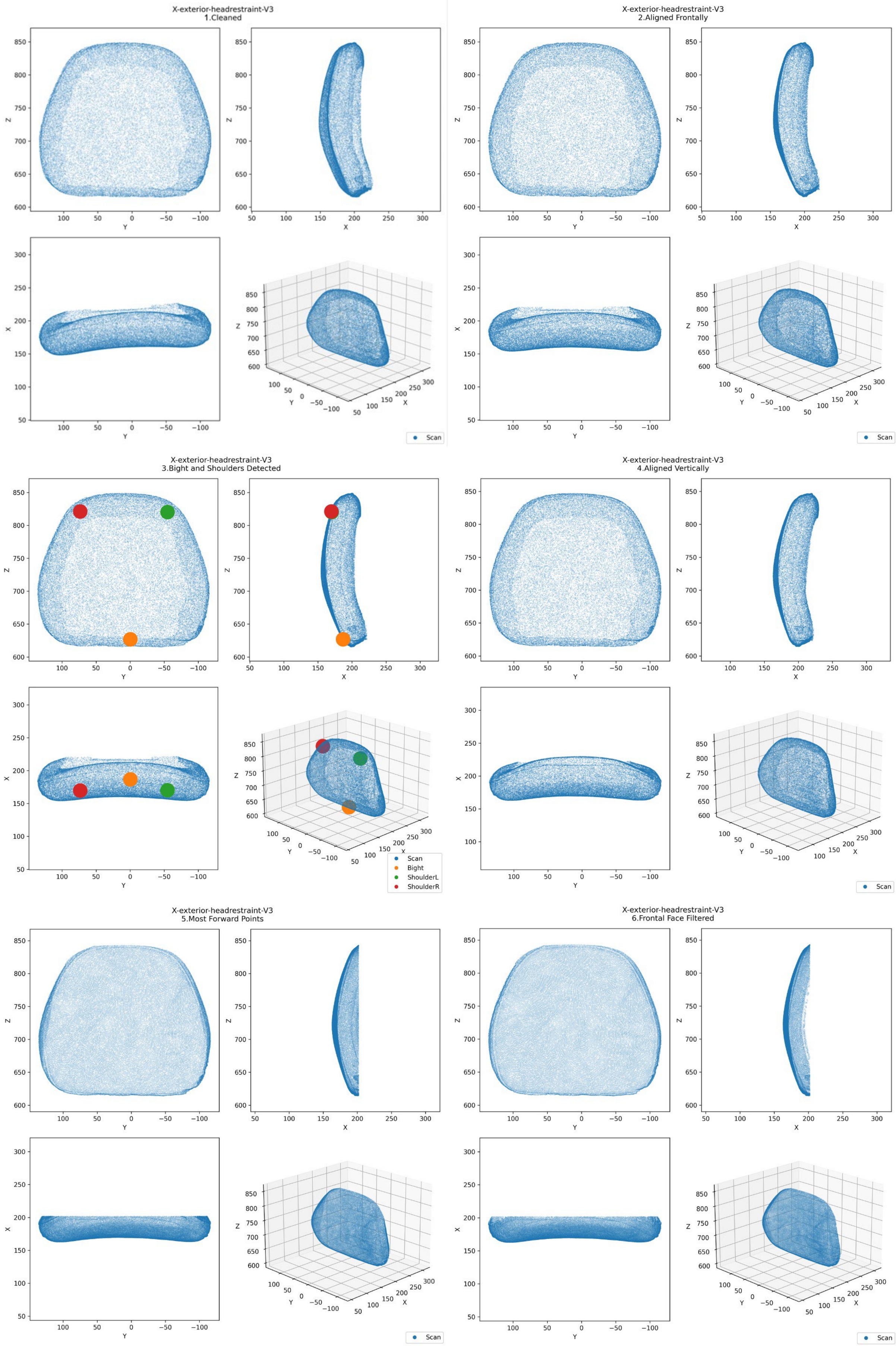

Fig. A1. Point Cloud Standardisation for Head Restraints (1).

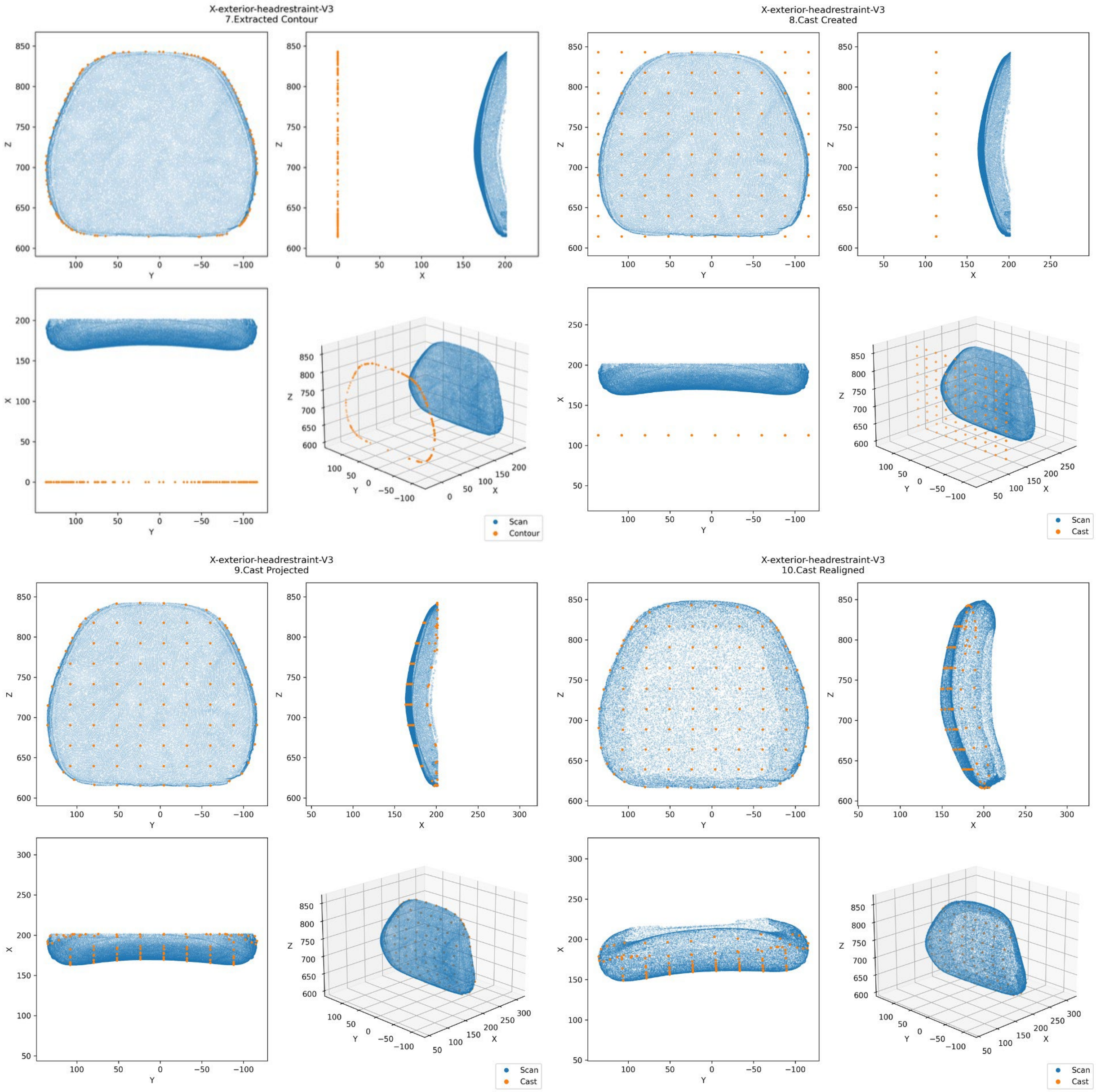

Fig. A2. Point Cloud Standardisation for Head Restraints (2).

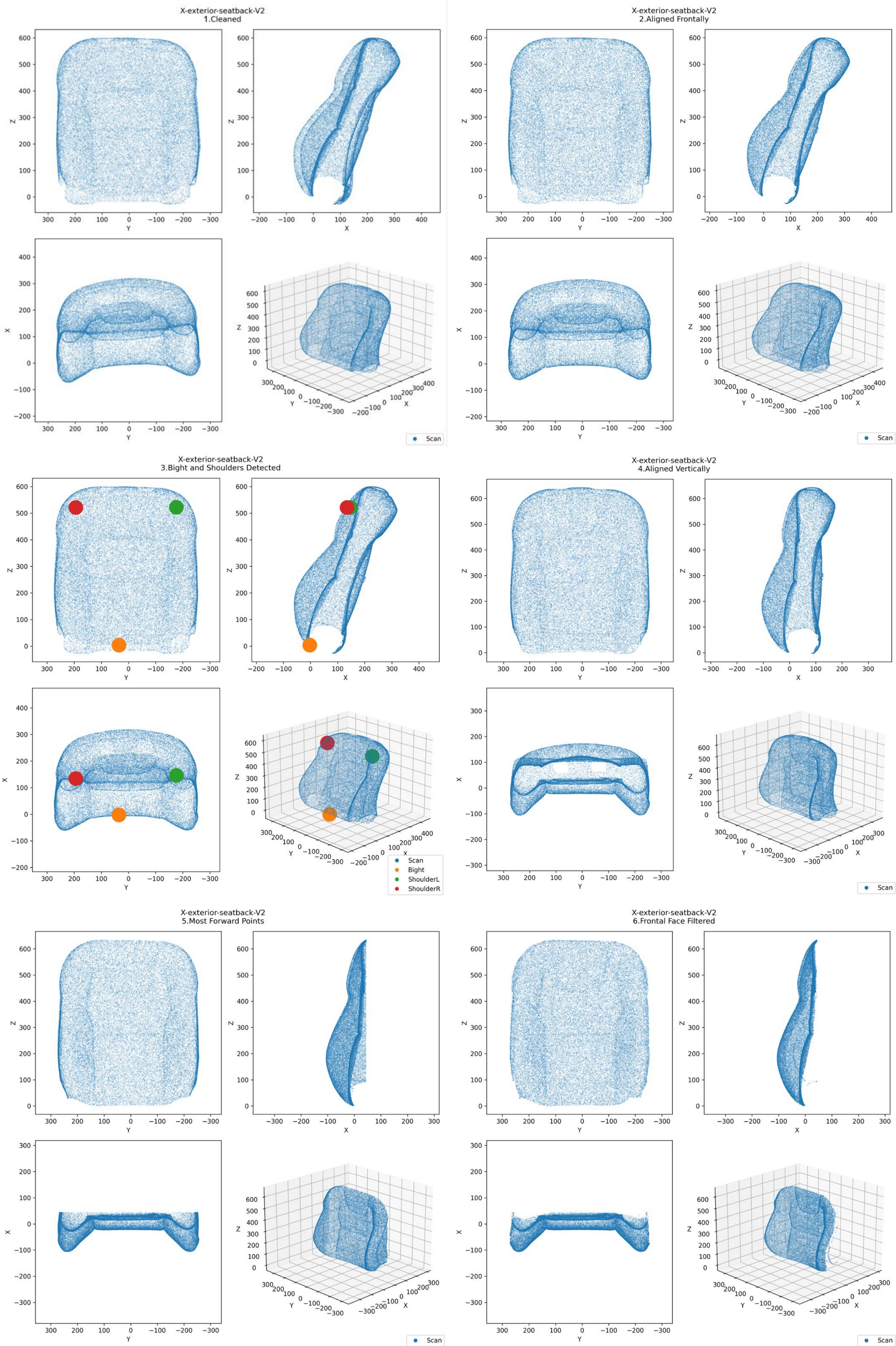

Fig. A3. Point Cloud Standardisation for Seat backs (1).

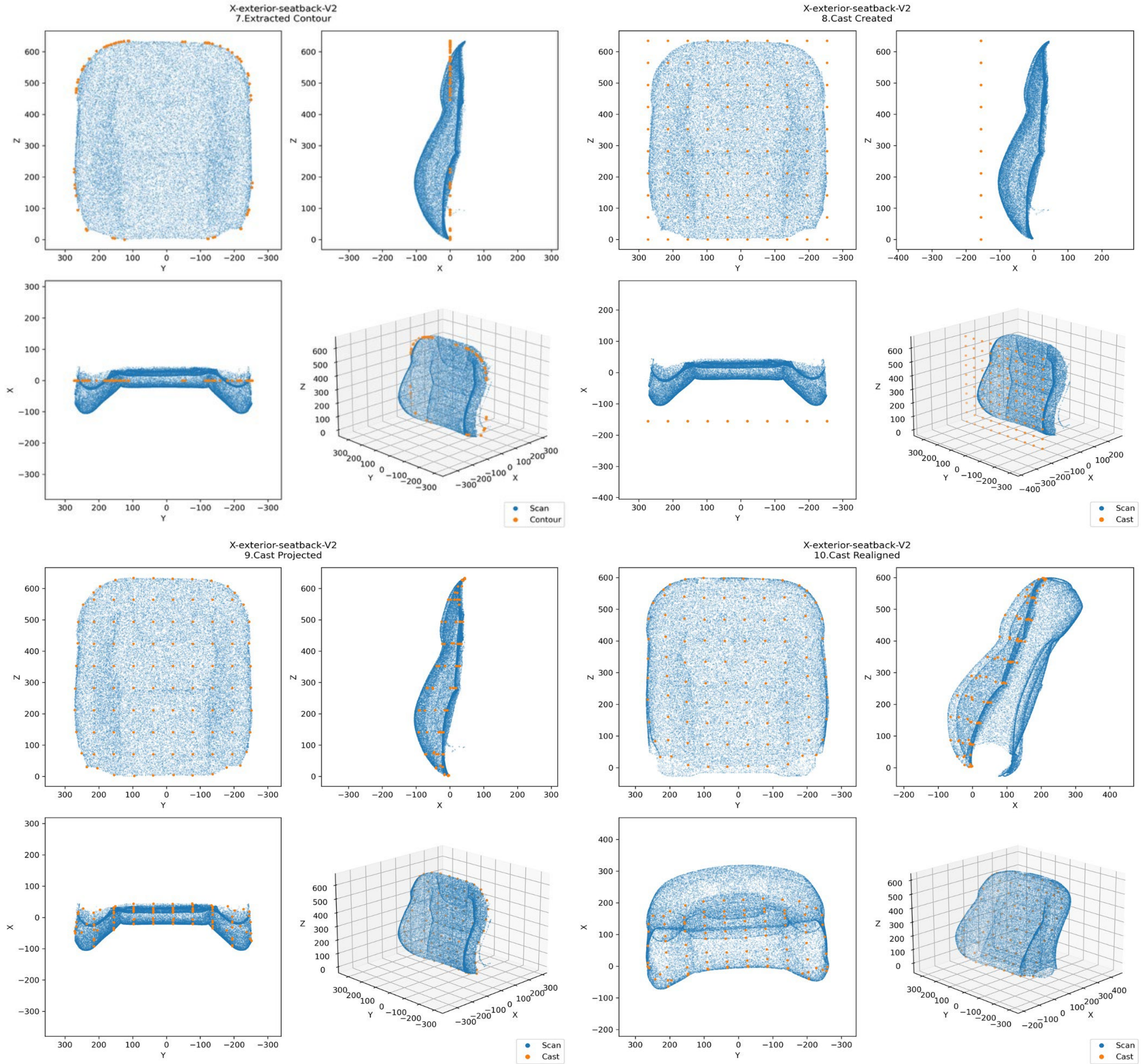

Fig. A4. Point Cloud Standardisation for Seat backs (2).

Appendix B: Seat morphing procedure

Fig. B1. Seat morphing procedure (1).

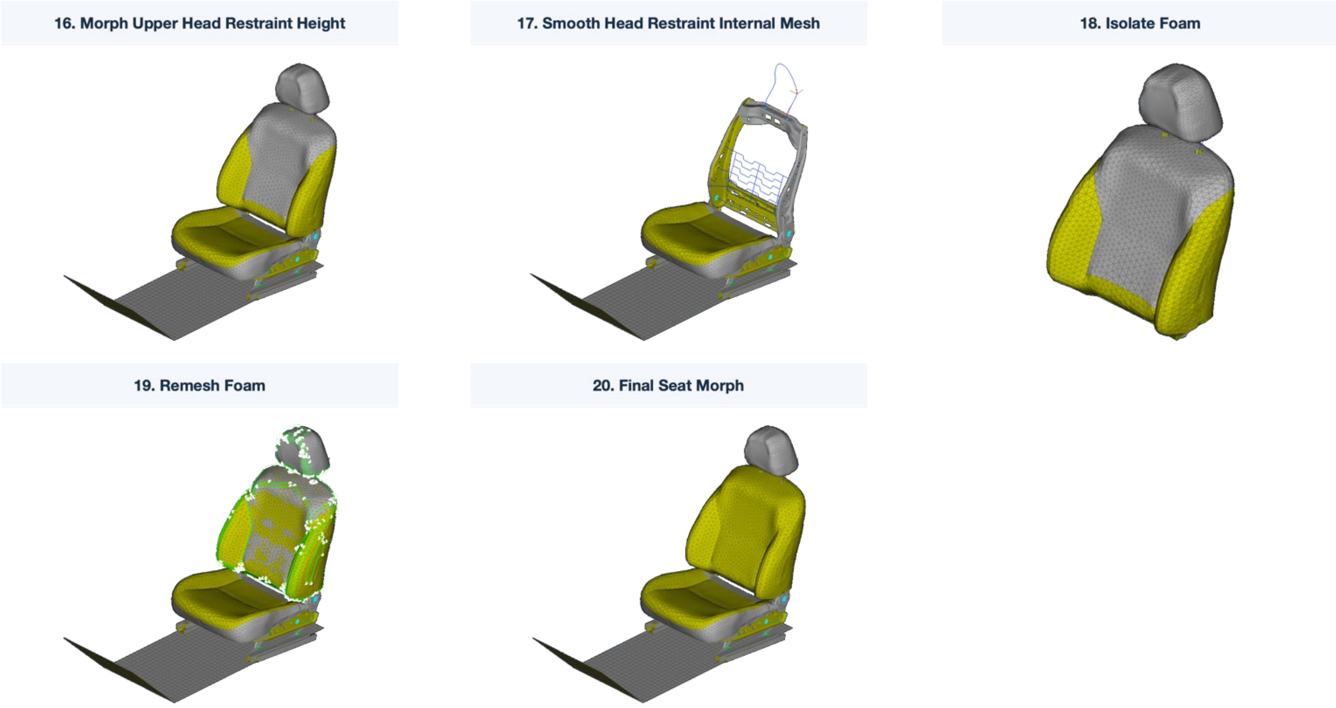

Fig. B2. Seat morphing procedure (2).

Appendix C: PCA Scree Plots

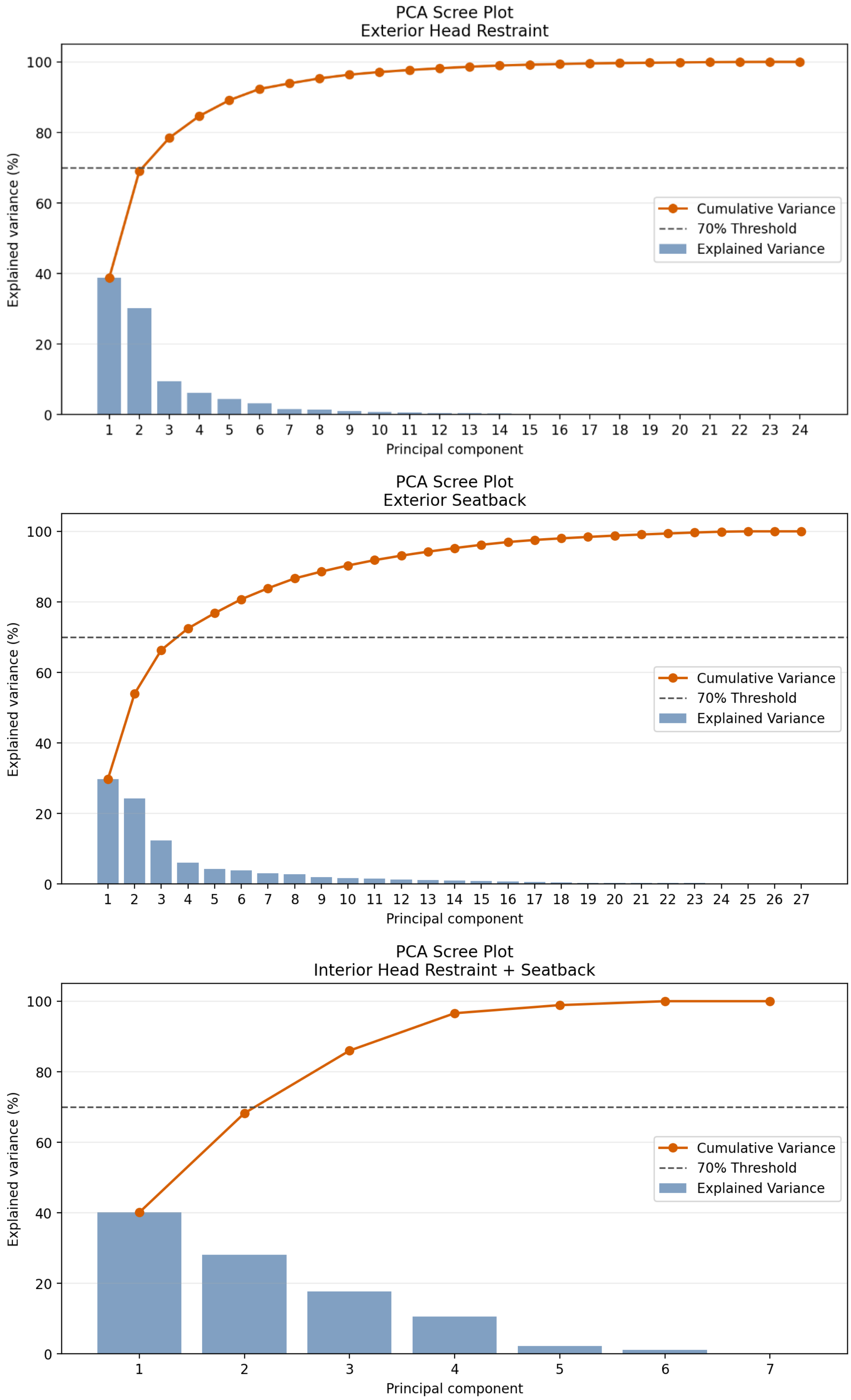

Fig. C1. PCA Scree plots.

Appendix D: PCA Mode Shapes

Each mode is shown over the same ±1 standard deviation range used for target generation, although the exercised generated seats combine multiple modes simultaneously.

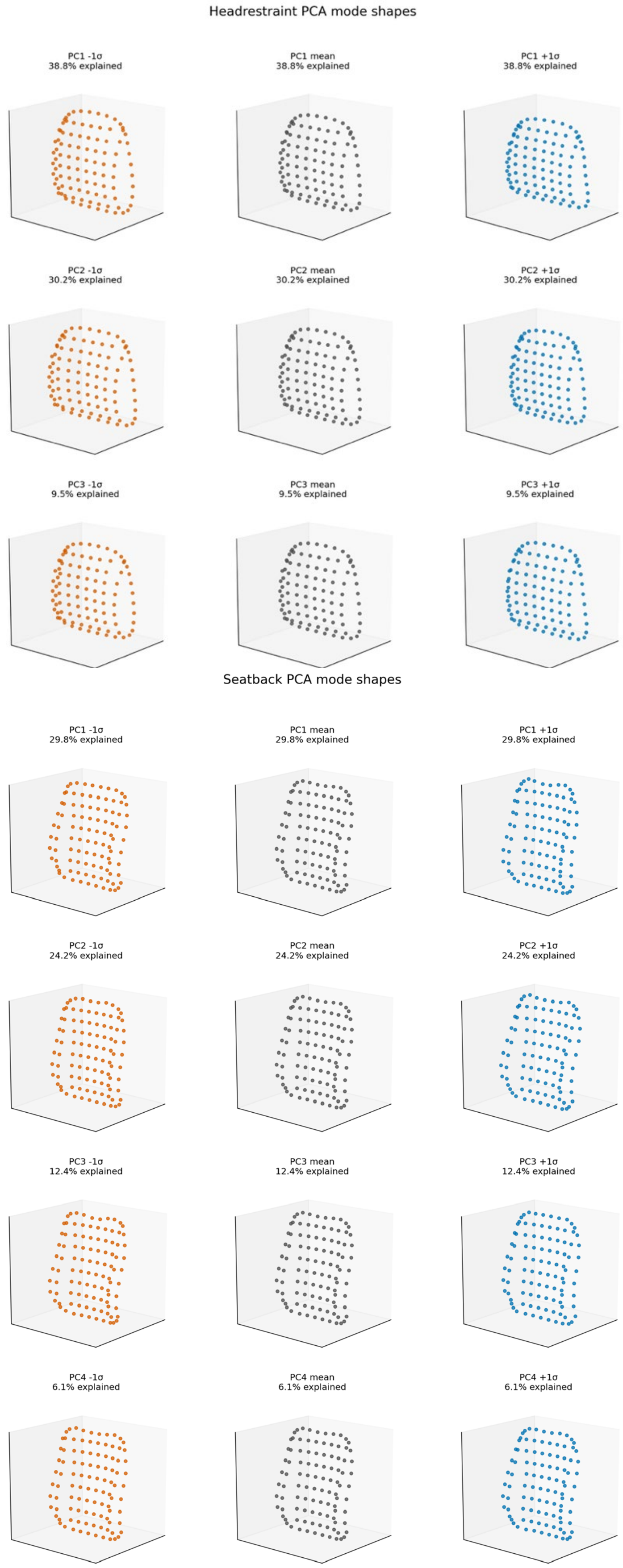

Fig. D1. PCA mode shapes for exterior seat back and head restraint.

Appendix E: PCA Reconstruction Plots

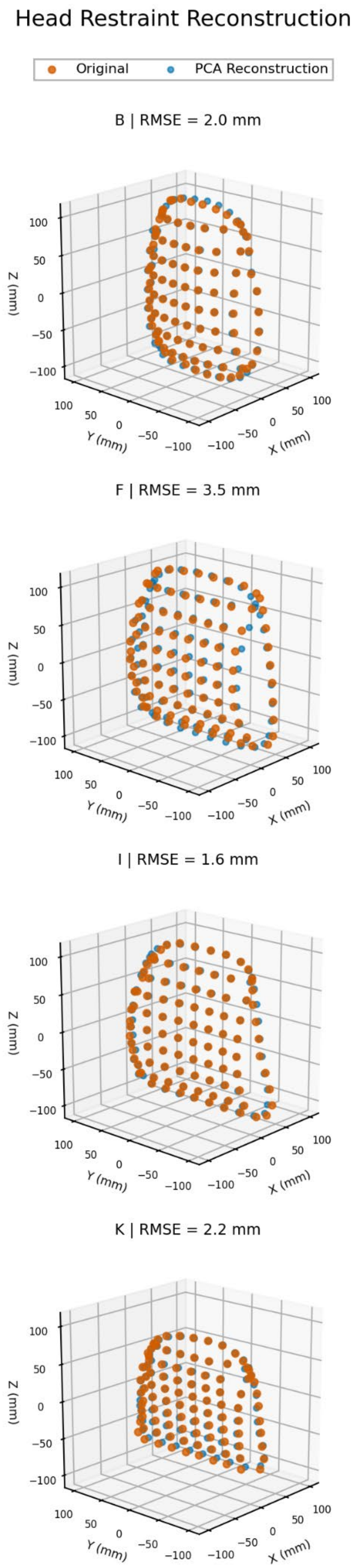

Fig. E1. Head restraint PCA reconstruction plot.

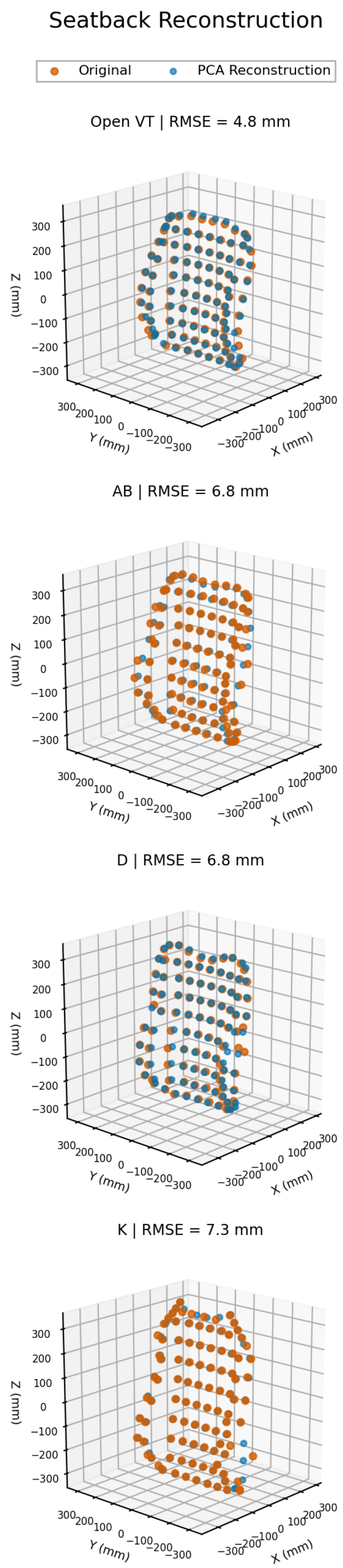

Fig. E2. Seat-back PCA reconstruction plots.